A numerical procedure to identify vugs and fractures in rock samples based on CT scan data

Victor M. Villegas[1], Yan Lobo[2], Nathan Shauer[3], Philippe R.B. Devloo [3]

[1]*Master program in mechanical engineering -Universidade Estadual de Campinas*
R. Josiah Willard Gibbs 85, Cidade Universitaria, 13083-841, Campinas-SP, Brazil
v272594@unicamp.br
[2]*Graduate program in civil engineering -Universidade Estadual de Campinas*
R. Josiah Willard Gibbs 85, Cidade Universitaria, 13083-841, Campinas-SP, Brazil
y195649@unicamp.br
[3]*LabMeC-FECFAU-Universidade Estadual de Campinas*
R. Josiah Willard Gibbs 85, Cidade Universitaria, 13083-841, Campinas-SP, Brazil
shauer@unicamp.br, phil@unicamp.br

Abstract. This article introduces novel algorithms for fractures and vugs recognition in computed tomography (CT) rock images. Although initial efforts focused on 2D images, the approach has the potential to be extended to 3D datasets with minimal modifications. A summarized explanation of the implemented method is provided, elucidating the underlying principles of the algorithms. Furthermore, the method's applicability is investigated through testing with various models of pre-trained convolutional neural networks and a K-nearest classifier. The study contributes to rock image analysis by introducing effective techniques for identifying fractures and vugs in CT scans that can be applied for geological and engineering purposes. In a demonstrative application, this methodology is implemented to generate a two-dimensional finite element mesh, with the objective of simulating a Darcy flow problem using the Finite Elements Method.

Keywords: Fracture, Vug, Computed tomography rocks, Shape descriptors , Flow simulation

1 Introduction

The identification of fractures and vugs in computed tomography (CT) rock images is essential for various geological and engineering applications, as noted by Li et al. [1]. Accurate detection of these features offers important insights into the structural integrity and fluid flow properties of rock formations. Traditional methods, often relying on manual inspection, are time-consuming and prone to errors, as highlighted by Elkhoury et al. [2]. To address these limitations, this paper proposes the use of shape descriptors for the automated recognition of fractures and vugs in CT rock images.

The proposed methodology utilizes pre-trained Convolutional Neural Networks (CNNs) of the Python library Pytorch [3] and shape descriptors to classify the images, which were implemented using Python library Numpy of Oliphant et al. [4] . Although initial efforts focused on 2D images, the approach has the potential to be extended to 3D datasets with further modifications. As noted by Wang et al. [5], employing advanced image processing techniques and machine learning models can significantly improve the accuracy and efficiency of feature identification.

This study assesses the adaptability of the proposed method by comparing it with different pre-trained neural network models. The effectiveness of the approach is evaluated using a standardized testing dataset. An illustrative example demonstrates the construction of a two-dimensional finite element mesh, which enables the simulation of fluid flow through identified fracture and vug networks using the Finite Elements Method (FEM).

2 Methodology

Figure 1 shows the workflow for classifying fractures and vugs, which starts with data acquisition, preprocessing, normalization, and splitting into training and testing sets. A total of 500 training images for each class, 100 validation images, and 50 test images were considered, totaling 1300 images. The pretrained Convolutional

Neural Network (CNN) Resnet first proposed by He et al. [6] and used for rocks computer vision analysis by Song et al. [7] was selected for the classification task, including hyperparameter tuning, training, and evaluation. Simultaneously, a K-Nearest Neighbors (KNN) classifier, an algorithm introduced in Cheng et al. [8] with n=5 uses the shape parameters extracted from the images. Both models outputs classified the images indicating fractures (0) and vugs (1).

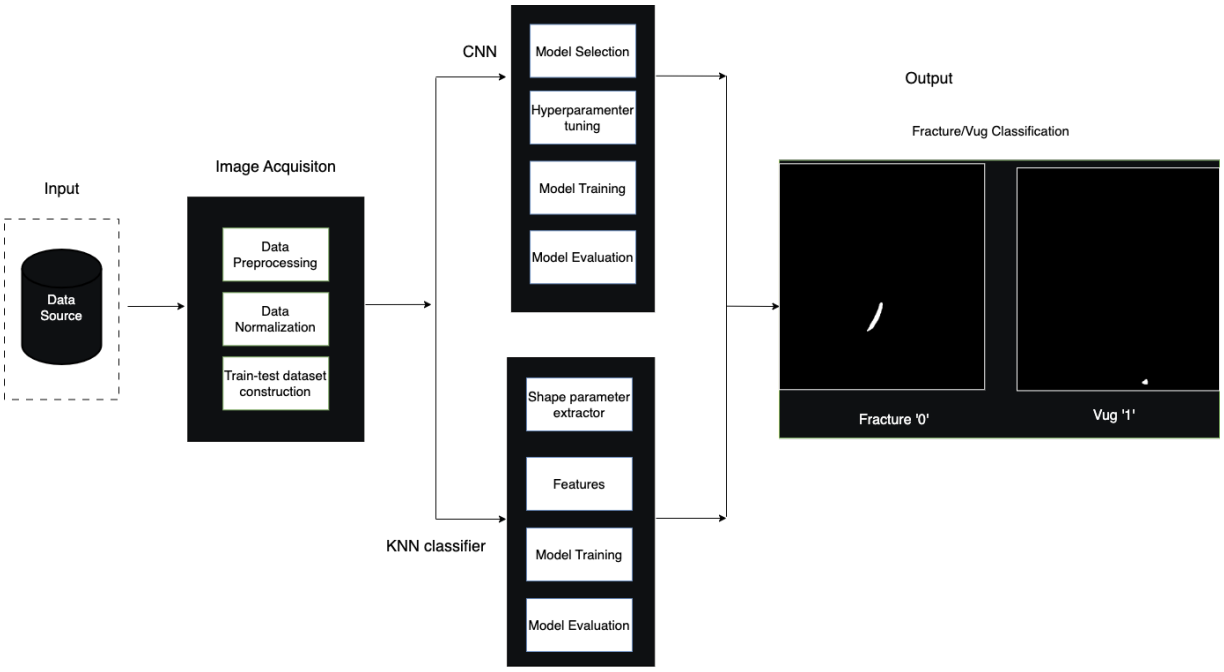

Figure 1. Workflow of the proposed study.

2.1 Shape Descriptors

Different shape descriptors have been used in the literature to characterize particles geometries, considering the ones from Jia et al. [9] and Li et al. [10].The equation used for calculating Convexity is given by:

$$C = \frac{A}{A_{Co}} \tag{1}$$

Where A is the total area and A_{Co} is the convex area.

The equation used for calculating Radial Variance is given by:

$$\sigma^2 = \frac{\sum_{i=1}^{n}(d_i - \bar{d})^2}{N} \tag{2}$$

Where d_i is the distance of the i-th point from the center, $\bar{d}$ is the mean distance, and N is the number of points.

The Area Sphericity is given by:

$$S_A = \frac{A}{A_{mC}} \tag{3}$$

Where A is the total area and A_{mC} is the area of the minimum circumscribed circle.

The Diameter Sphericity is given by:

$$S_D = \frac{D}{D_{mC}} \tag{4}$$

Where D is the diameter of the figure and D_{mC} is the diameter of the minimum circumscribed circle.

The Surface Area Sphericity is given by:

$$S_{SA} = \frac{A_{mC}}{A_{mE}} \tag{5}$$

Where A_{mC} is the area of the minimum circumscribed circle and A_{mE} is the area of the minimum circumscribed ellipse. This size parameters are illustrated in Fig. 2.

The Aspect Ratio is given by:

$$R_A = \frac{LEN_{min}}{LEN_{max}} \tag{6}$$

Where LEN_{min} is the minimum length represented with the red line in the left figure of Fig. 2 and LEN_{max} is the maximum length represented with the blue line in the left figure of the same figure.

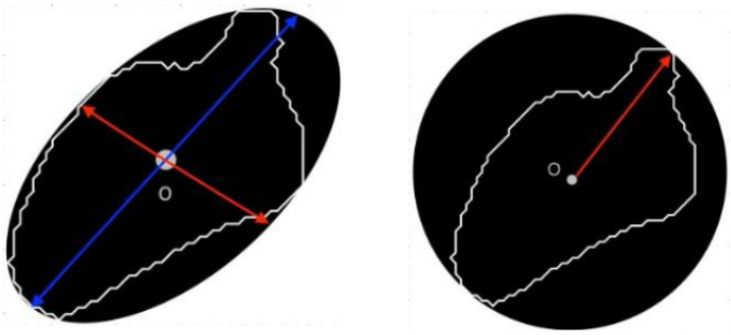

Figure 2. Some size descriptors.

2.2 Numerical Example

From Fig. 3 red bounding boxes, some geometries were extracted and segmented in Fig. 4. The shape descriptors of them are shown in Table 1 . This size parameters were obtained using OpenCV library proposed by Bradski [11].

As an example of the process used to calculate the shape parameters, those parameters are calculated for the fourth geometry of Fig. 4:

Convexity is calculated using eq. (1):

$$C = \frac{171919.0}{2296.5} \approx 0.7485$$

Radial variance is given by eq. (2). Radial variance is also dimensionless, and the result is 31.17.

Area sphericity is calculated using eq. (3):

$$S_A = \frac{1719.0}{\pi \cdot 36.17^2} \approx 0.4181$$

Diameter sphericity is dimensionless, calculated as the ratio between the equivalent diameter and the diameter of the minimum circumscribed ellipse. The equivalent diameter of the figure is obtained from its area using:

$$D_{equiv} = 2\sqrt{\frac{1719.0}{\pi}} = 46.78$$

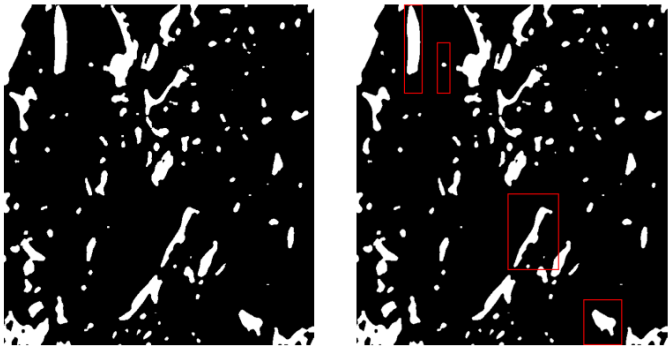

Figure 3. An example of CT scan.

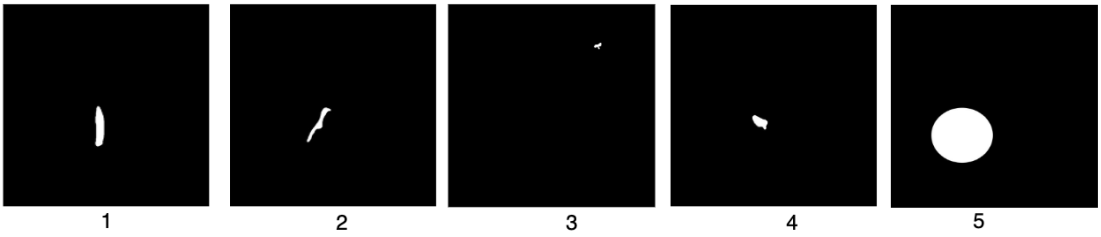

Figure 4. Some geometries of CT scan to be analyzed.

where the area of the figure is the area of the considered figure. This parameter provides a measure of how circular the figure is, with a value of 1 indicating a perfectly circular figure and lower values indicating deviations from circularity. Diameter sphericity is calculated using eq. (4):

$$S_D = \frac{46.78}{2 \cdot 36.17} \approx 0.646$$

Surface area sphericity is calculated using eq. (5):

$$S_{SA} = \frac{\pi(36.17)^2}{\frac{\pi(65.41)^2}{4}} \approx 1.442$$

Aspect ratio is calculated using eq. (6):

$$R_A = \frac{30.32}{65.41} \approx 0.596$$

Aspect ratio as the other shape parameters is dimensionless. Previously, geometries were analyzed in two dimensions. However, using this methodology, it is possible to characterize each plane of a 3D geometry individually, determining whether the candidate is a fracture or a vug based on the same principles. This approach allows for a comprehensive analysis of 3D structures by examining each 2D slice sequentially. In Fig. 5 it is possible to see a 3D connected component, and on the right a 2D projection of it.

3 Results and discussion

The proposed methodology aims to automate the identification of fractures and vugs in CT rock images. Our approach leverages pre-trained Convolutional Neural Networks (CNNs) and shape descriptors to classify these features. Despite initial efforts, we observed that the CNN model, specifically Resnet, did not show a clear trend towards convergence during the training epochs for 2D images in Fig. 6. This lack of convergence suggests that the CNN approach may not be best suitable for this specific task without further adjustments or enhancements.

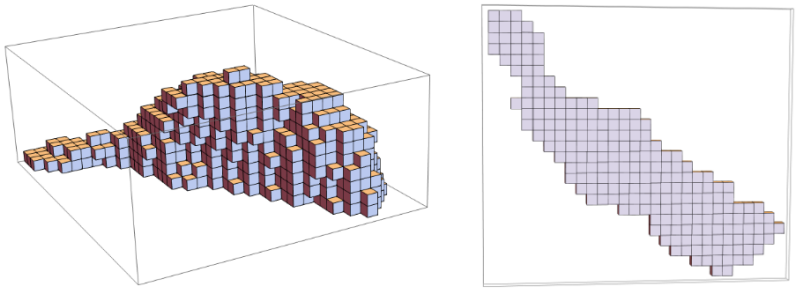

Figure 5. 3D Methodology extension.

Table 1. Morphological Parameters of 2D Geometries (First fourth parameters have units of pixels)

Parameter	Geometry 1	Geometry 2	Geometry 3	Geometry 4	Geometry 5
Perimeter (pix)	525.81	745.11	66.18	413.33	3540
Major Ellipse Axis	145.85	132.75	14.49	65.41	466.21
Minor Ellipse Axis	34.867	30.32	8.18	38.96	465.28
Minimum Circle Radius	71.56	67.79	7.915	36.17	238.684
Area (pix^2)	280	2299.0	43	1719.0	2177
Convexity	0.865	0.5542	0.751	0.749	0.96
Radial Variance	240.54	300.38	4.14	31.17	4.11
Area Sphericity	0.222	0.159	0.264	0.418	0.94
Diameter Sphericity	0.471	0.399	0.514	0.647	0.97
Surface Area Sphericity	3.619	3.183	1.254	1.442	0.99
Aspect Ratio	0.239	0.228	0.454	0.596	0.998

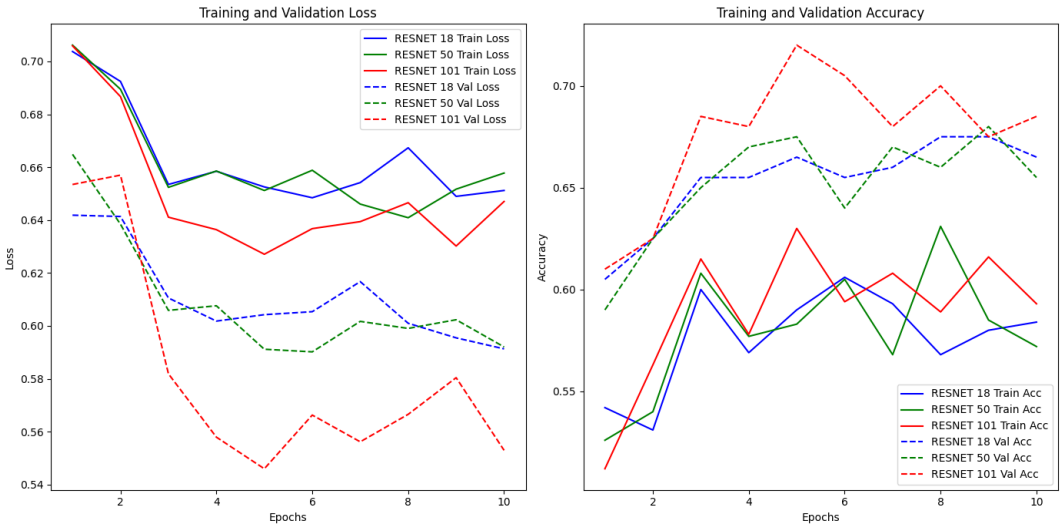

Figure 6. CNN-Resnet training results.

In contrast, our experiments with shape descriptors and K-Nearest Neighbors (KNN) classifiers demonstrated more promising results. By directly utilizing calculated shape parameters, the KNN classifier achieved better performance in classifying fractures and vugs as in can be see in Table 2. This improvement underscores the importance of feature selection and efficient preprocessing; choosing the right shape descriptors is crucial for

accurate classification. A dispersion diagram for two shape parameters is shown in Fig. 7 which shows how the two classes are concentrated in high values of aspect ratio and convexity for vugs and in lower values for fractures.

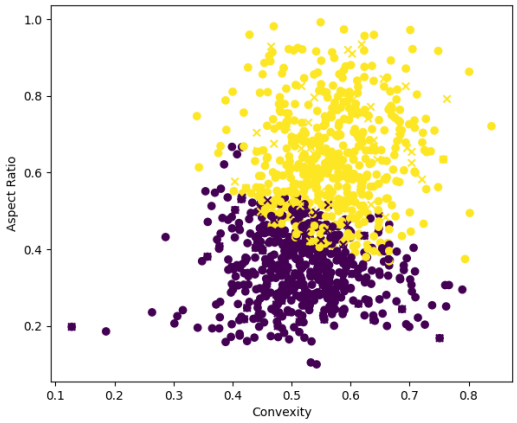

Figure 7. Illustrative dispersion diagram of K-NN classification.

Table 2. KNN Metrics Summary.

Metric	Training Set	Test Set
Accuracy	0.90	0.89
Precision	0.92	0.92
Recall	0.88	0.86
F1-Score	0.90	0.89

3.1 Next steps

An important application of this study is in the simulation of porous media flow through rock samples. By accurately identifying simple vugs and fractures, the generated 2D finite element meshes can be employed in simulating physical processes using the Finite Elements Method (FEM). This simulation capability is crucial for geological and engineering analyses. As an example of the applicability of the study, we utilized the NeoPZ library [12] to configure an initial case considering all possible vug and fracture candidates as voids within the domain. The approximation space H^1 was adopted with no-flow boundary conditions on the top and bottom surfaces.The results from this simulation are depicted in Fig. 8.

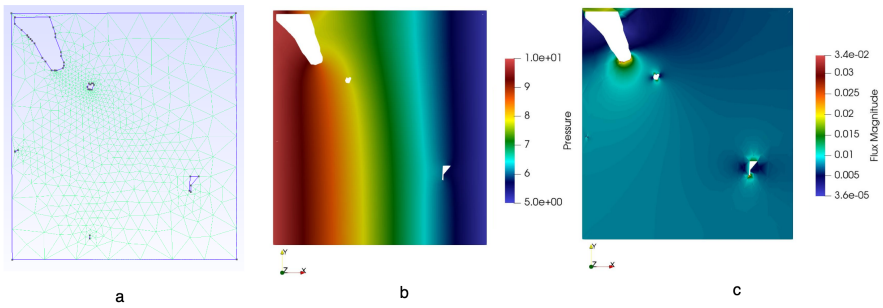

Figure 8. Initial case of applicability.

This initial case serves as a foundation for more complex simulations. Future work will involve incorporating

Discrete Fracture Network (DFN) systems to more accurately represent and simulate the intricate network of fractures present in rock formations.

4 Conclusions

Some of the most important key findings include that the Resnet model did not demonstrate effective convergence during training epochs for 2D images, suggesting limitations in using CNNs for this specific task without further adjustments. Experiments with shape descriptors and K-Nearest Neighbors (KNN) classifiers provided better classification results. The direct use of calculated shape parameters improved the accuracy of identifying fractures and vugs. The importance of robust feature selection was underscored, as choosing the appropriate shape descriptors was crucial for accurate classification. Future work will focus on incorporating Discrete Fracture Network (DFN) systems to simulate more complex geological scenarios. By integrating DFN systems, the methodology aims to enhance simulation capabilities, allowing for comprehensive analyses of fluid flow and structural integrity in geologically complex formations. Efforts will also be directed towards improving classification accuracy for 3D datasets.

Acknowledgements. We express our sincere gratitude to the Coordination for the Improvement of Higher Education Personnel (CAPES), the National Council for Scientific and Technological Development (CNPq), the São Paulo Research Foundation (FAPESP), the Center for Petroleum Studies (CEPETRO), School of Mechanical Engineering (FEM), and the School of Civil Engineering, Architecture and Urban Planning (FECFAU) of the University of Campinas (UNICAMP) for their generous support.

Authorship statement. The authors hereby confirm that they are the sole liable persons responsible for the authorship of this work, and that all material that has been herein included as part of the present paper is either the property (and authorship) of the authors, or has the permission of the owners to be included here.

References

[1] B. Li, X. Tan, F. Wang, P. Lian, W. Gao, and Y. Li. Fracture and vug characterization and carbonate rock type automatic classification using x-ray ct images. *Journal of Petroleum Science and Engineering*, vol. 153, pp. 88–96, 2017.

[2] J. E. Elkhoury, R. Shankar, and T. Ramakrishnan. Resolution and limitations of x-ray micro-ct with applications to sandstones and limestones. *Transport in Porous Media*, vol. 129, n. 1, pp. 413–425, 2019.

[3] A. D. I. Pytorch. Pytorch, 2018.

[4] T. E. Oliphant and others. *Guide to numpy*, volume 1. Trelgol Publishing USA, 2006.

[5] Y. Wang, Q. Teng, X. He, J. Feng, and T. Zhang. Ct-image of rock samples super resolution using 3d convolutional neural network. *Computers & Geosciences*, vol. 133, pp. 104314, 2019.

[6] K. He, X. Zhang, S. Ren, and J. Sun. Deep residual learning for image recognition. In *Proceedings of the IEEE conference on computer vision and pattern recognition*, pp. 770–778, 2016.

[7] Z. Song, Z. Zhang, G. Zhang, J. Huang, and M. Wu. Identifying the types of loading mode for rock fracture via convolutional neural networks. *Journal of geophysical research: solid Earth*, vol. 127, n. 2, pp. e2021JB022532, 2022.

[8] D. Cheng, S. Zhang, Z. Deng, Y. Zhu, and M. Zong. k nn algorithm with data-driven k value. In *Advanced Data Mining and Applications: 10th International Conference, ADMA 2014, Guilin, China, December 19-21, 2014. Proceedings 10*, pp. 499–512. Springer, 2014.

[9] X. Jia, R. Liu, H. Ren, Y. Han, J. Ouyang, H. Zheng, C. Peng, and J. Zheng. Particle shape characterizations for energetic materials by computational geometry and stereology method. *SN Applied Sciences*, vol. 4, n. 5, pp. 147, 2022.

[10] X. Li, J. Shen, W. Yang, and Z. Li. Automatic fracture–vug identification and extraction from electric imaging logging data based on path morphology. petroleum science, 16 (1). *Crossref Web of Science*, 2019.

[11] G. Bradski. The opencv library. *Dr. Dobb's Journal: Software Tools for the Professional Programmer*, vol. 25, n. 11, pp. 120–123, 2000.

[12] P. R. Devloo. Object oriented tools for scientific computing. *Engineering with computers*, vol. 16, pp. 63–72, 2000.